Influence of nitrogen and magnesium doping on the properties of ZnO films*

Dong-hua Li(李东华)[1], Hui-Qiong Wang(王惠琼)[1,2,3,†], Hua Zhou(周华)[1], Ya-Ping Li(李亚平)[1], Zheng Huang(黄政)[1], Jin-Cheng Zheng(郑金成)[1,2], Jia-Ou Wang(王嘉鸥)[4], Hai-jie Qian(钱海杰)[4], Kurash Ibrahim(奎热西)[4], Xiaohang Chen(陈晓航)[1], Huahan Zhan(詹华瀚)[1], Yinghui Zhou(周颖慧)[1], and Junyong Kang(康俊勇)[1]

[1] *Fujian Provincial Key Laboratory of Semiconductors and Applications, Collaborative Innovation Center for Optoelectronic Semiconductors and Efficient Devices, Department of Physics, Xiamen University, Xiamen* 361005, *China*

[2] *Xiamen University Malaysia Campus, Sepang, Selangor* 439000, *Malaysia*

[3] *State Key Laboratory of Silicon Materials, Zhejiang University, Hangzhou* 310027, *China*

[4] *Beijing Synchrotron Radiation Facility, Institute of High Energy Physics, Chinese Academy of Sciences, Beijing* 100049, *China*

(Received 28 December 2015; revised manuscript received 2 March 2016; published online 30 May 2016)

Undoped ZnO and doped ZnO films were deposited on the MgO(111) substrates using oxygen plasma-assisted molecular beam expitaxy. The orientations of the grown ZnO thin film were investigated by *in situ* reflection high-energy electron diffraction and *ex situ* x-ray diffraction (XRD). The film roughness was measured by atomic force microscopy, which was correlated with the grain sizes determined by XRD. Synchrotron-based x-ray absorption spectroscopy was performed to study the doping effect on the electronic properties of the ZnO films, compared with density functional theory calculations. It is found that, nitrogen doping would hinder the growth of thin film, and generate the N_O defect, while magnesium doping promotes the quality of nitrogen-doped ZnO films, inhibiting $(N_2)_O$ production and increasing nitrogen content.

Keywords: ZnO, nitrogen, magnesium, x-ray absorption spectra

PACS: 61.72.uj, 61.05.cj, 61.05.js **DOI:** 10.1088/1674-1056/25/7/076105

1. Introduction

The semiconductor ZnO has gained substantial interest in the research community partly because of its potential application in ultraviolet photoelectric devices,[1] which was due to its direct and wide band gap with a large exciton binding energy (60 meV).[2] However, the application of ZnO in optoelectronics is hindered by the lack of a stable p-doping because of the native defect: the O vacancy (V_O) and the Zn interstitial (i_{Zn}),[3] or hydrogen doping in ZnO.[4] Many methods have been carried out to fabricate p-type ZnO by doping of group-V (N, P, As, Sb)[5–7] and group-I [Li],[8] among which, N is predicted to be an outstanding dopant candidate,[9] but the real application is unfortunately limited by its low solubility in ZnO. On the other hand, it has been suggested by the calculation that Mg could improve the solubility of nitrogen in the ZnO.[10] However, there is very little experimental research on the N, Mg co-doped ZnO. We therefore investigated the co-doping effect of Mg and N in ZnO, comparing with those ZnO films without doping or with sole N-doping.

2. Experiments and calculations

The MgO substrates were first degreased by ultrasonic bath in acetone, followed by ethanol. After being introduced into the MBE growth chamber (ultra-high vacuum environment, with a base pressure of 10^{-9} mbar), the substrates were annealed at 400 °C for 60 min while the power of the radio frequency plasma source was set to 250 W and the oxygen partial pressure maintained at 5×10^{-5} mbar. The substrates were then further treated with 5 repeated treatment circles using N_2 plasma and Mg beam sequentially, followed by the growth of the ZnO buffer films with the temperature of elemental zinc source (with a purity of 99.9999%) maintained at 330 °C, the substrate temperature at 300 °C and the oxygen partial pressure kept at 1×10^{-5} mbar with the power of plasma source at 250 W. For the subsequent growth of N-doped ZnO films with or without Mg dopants, the N_2 pressure was kept at 5×10^{-5} mbar. For the growth of N-doped ZnO films with Mg dopants, the temperature of elemental magnesium (with a purity of 99.9999%) was maintained at 350 °C. *In situ* reflection high-energy electron diffraction (RHEED) was used to monitor the process of ZnO growth. The film roughness was characterized by atomic force microscopy (AFM). The crystalline structure was characterized by x-ray diffraction (XRD, Cu anode $\lambda_{K\alpha_1} = 1.54056$ Å), the chemical composition was determined by x-ray photoelectron spectroscopy (XPS) and the electronic structures of the

*Project supported by the National Natural Science Foundation of China (Grant Nos. 11204253, U1332105, 61227009, and 91321102), the Fundamental Research Funds for Central Universities, China (Grant No. 20720160020), and the National High Technology Research and Development Program of China (Grant No. 2014AA052202).

†Corresponding author. E-mail: hqwang@xmu.edu.cn

© 2016 Chinese Physical Society and IOP Publishing Ltd

thin films were probed by synchrotron-based x-ray absorption spectroscopy (XAS). To compare with XAS results, first principles calculations have been performed using WIEN2K codes,[11] and the Perdew–Burk–Ernzerhof (PBE) parameterization of the generalized gradient approximation (GGA)[12] is used for exchange–correlation potential. The band structure and density of states of N-doped and undoped ZnO are used to interpret the XAS results.

3. Results

3.1. Reflection high-energy electron diffraction

The morphology of the ZnO films grown on the MgO (111) substrates with different doping elements of N and Mg can be seen through the RHEED patterns captured *in situ* after the growth,[13] as shown in Fig. 1. Generally speaking, streaky RHEED patterns indicate a flat sample surface and the spots indicate poor consistency on the surface, while the spotty patterns indicate a three-dimensional feature. Figure 1(a) shows the RHEED pattern of the ZnO film without doping, along the [1-210] azimuth and the streaky feature indicates a growth mode close to two-dimensional. Figure 1(b) shows the RHEED pattern of the ZnO film with N doping. The RHEED pattern becomes dotty, indicating that N doping damages the two-dimensional growth of ZnO, which is consistent with the previous results.[14] Figure 1(c) shows the RHEED patterns of the ZnO film with co-doping of N and Mg elements. It also exhibits a spotty feature, sharper than those in Fig. 1(b), indicating that Mg may promote the growth of N-doped ZnO thin film. Both RHEED patterns in Figs. 1(b) and 1(c) show a small extension along the [1-210] azimuth, implying a smaller coherence on the surface.

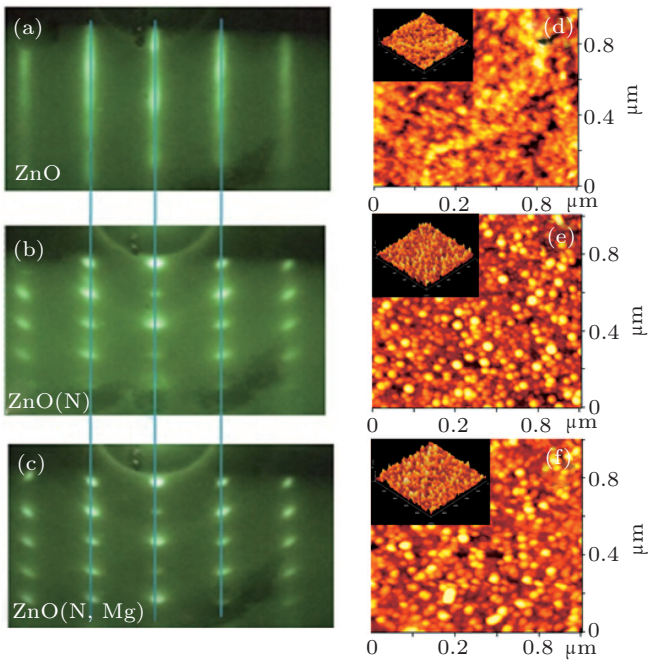


Fig. 1. (color online) (a) RHEED pattern of the ZnO film along the [1-210] azimuth, grown on the MgO (111) substrate. (b) RHEED pattern of the ZnO film surface with N doping. (c) RHEED pattern of the ZnO film surface with co-doping of N and Mg. (d) AFM images of ZnO without doping (e) AFM images of ZnO with N doping and (f) AFM images of ZnO with N, Mg co-doping.

3.2. Atomic force microscopy

Such an effect is further proved by the AFM images captured from these three film samples, as shown in Fig. 1. The ZnO film without doping shows a relatively smoother morphology (Fig. 1(d)), with an RMS value of 0.60 nm, while N doping induces an island structure (Fig. 1(e)) with an RMS value of 3.46 nm. For the ZnO film with N and Mg co-doping, the AFM image (Fig. 1(f)) shows a decrease of the RMS value to 2.70 nm.

3.3. The x-ray diffraction

The phase structures of the grown undoped and doped ZnO films were measured by XRD, as shown in Fig. 2. The 2θ values in x axis of Fig. 2 are calibrated by the substrate signal, (i.e., the strong peaks at 37.02° observed before growth of ZnO, which is illustrated in Fig. 2). All three films exhibit a feature at around 34.6°, assigned to ZnO (002). The presence of such a strong ZnO (002) feature, compared to other ZnO features, indicate that the deposited ZnO films are highly oriented. Further inspection of the XRD spectra shows that the position of ZnO (002) peaks shifts slightly after doping (i.e., the 2θ values of the peak for undoped, N-doped, and N–Mg co-doped ZnO films are 34.55°, 34.68°, and 34.66°, respectively). It is speculated that N hinders the growth of ZnO[15] and then prevents the complete relaxation of the stress, thus causing the excursion of the 2θ of ZnO (002) peak. The small diffraction peak at about 30.7° is likely originated from ZnO (100). It is also noted that, for the same

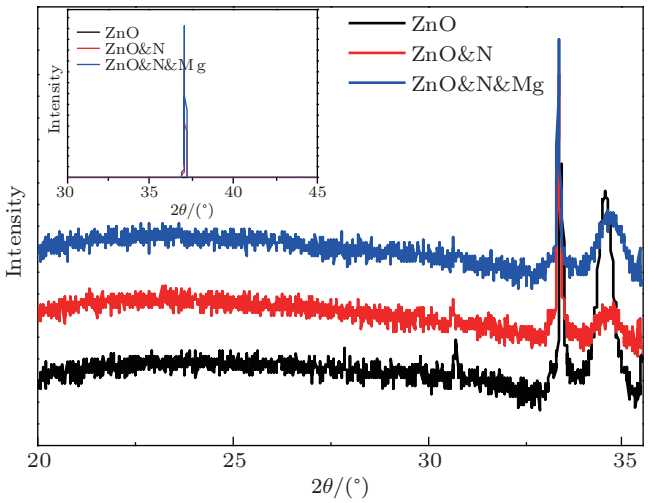


Fig. 2. (color online) The x-ray diffraction spectra of ZnO, N-doped ZnO, and N–Mg co-doped ZnO films. The inset shows the whole spectroscopy of samples.

growth parameters, the quality of the co-doped ZnO films is worse than that of the undoped ZnO film, as indicated by the lower intensity and larger FWHM of the ZnO (002) peak.

The average crystallite size (D) was estimated from the Debye–Scherrer's equation[16]

$$D = \frac{0.2\lambda}{\beta \cos\theta},$$

where λ represents the wavelength of the x-ray radiation, is the full width at half maximum (FWHM) of diffraction peak, and is the scattering angle. The crystallite size of the ZnO film, the N-doped ZnO film, and N–Mg co-doped ZnO film is 4.6 nm, 2.7 nm, 3.9 nm, respectively, indicating that Mg probably improves the quality of N-doped ZnO films and leads to a smoother morphology than the N-doped ZnO film without Mg doping.

3.4. The x-ray absorption spectroscopy

Figure 3(a) shows the synchrotron-based x-ray absorption spectra of the ZnO film (oxygen K-edge) with different incident angles, which shows an obvious polarization dependence with the photon energy higher than 535 eV, indicating that the features at 530–535 eV and above 535 eV could be attributed to the O 2p states that hybridize with the isotropic Zn 4s states and anisotropic Zn 4pd states, respectively.

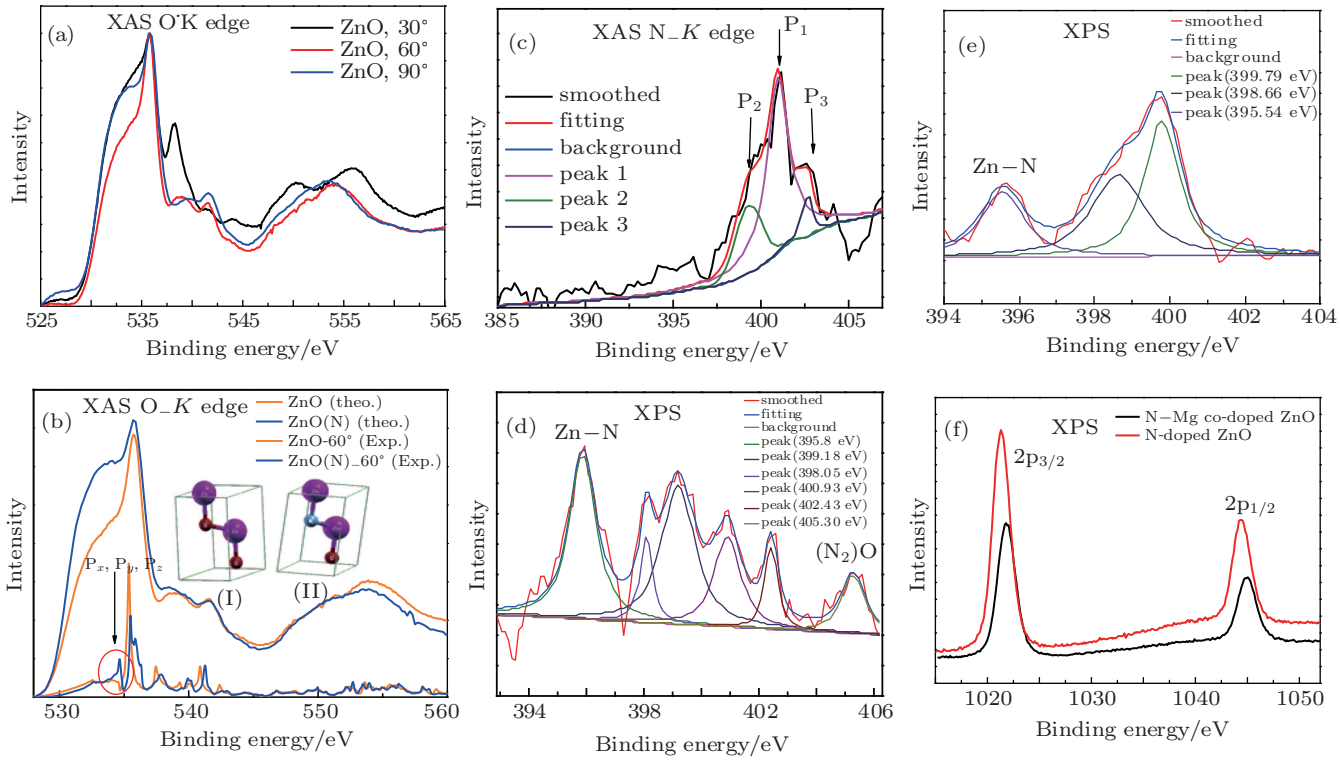


Fig. 3. (color online) The XAS spectra for O-K edge of ZnO at the incident angles of 30°, 60°, 90°; (b) XAS and DFT calculations results (PDOS) for ZnO with and without doping. The inset shows the atomic models (I) and (II), where the big atoms represent Zn atoms, the red atoms represent O atoms and the blue atoms represent N atoms. (c) The N-K edge spectrum of the ZnO with N doping sample at the incident angle of 40°. (d) The XPS spectrum for N-doped ZnO film. (e) The XPS spectrum of N–Mg co-doped ZnO film. (f) The XPS spectra of Zn2p$_{3/2}$ of N-doped ZnO and N–Mg co-doped ZnO films.

Figure 3(b) compares the experimental oxygen K-edge spectra of ZnO with and without N doping. The projected density of states (PDOS) from the DFT calculations are also shown (in the lower layer of Fig. 3(b)) with the atomic models illustrated in the inset. Significant differences between the spectra of ZnO with and without N doping can be observed, especially at the lower energy region. Features in the photon energy regions of 530–540 eV, 540–550 eV and above 550 eV are attributed to the hybridized states of O 2p–Zn 4s, O 2p–Zn 4p, and O 2p–Zn 4d, respectively.[17] The peak positions of the PDOS contributed by P_x, P_y, P_z orbitals are easily distinguished at about 7.6 eV above the Fermi level, which corresponds to the binding energy at about 534.7 eV. The peak at about 534 eV for the N-doped ZnO is higher than that for the ZnO without doping. This could be explained by the smaller number of valence electrons of N (5 electrons from $2s^2 2p^3$) than those of oxygen (6 electrons from $2s^2 2p^4$). When some oxygen sites in ZnO have been occupied by nitrogen atoms, less charges are transferred from Zn to nearby oxygen sites due to the interference of doped nitrogen. Thus, the oxygen

in N-doped ZnO has more unoccupied states than that in ZnO without doping. In the nitrogen *K*-edge spectrum as shown in Fig. 3(c), there is a strong resonant peak P_1 at 401 eV, which is the characteristic triple bonded N_2 bound state resonance, as well as a shape resonance in the continuum around 400.9 eV.[18] As metal nitrides have two sharp resonances at the photo energies ranging from 397.5 eV to 401.5 eV, assigned to the transitions of N 1s electrons to the p–d (t_{2g}) and p–d (e_g) hybridized orbitals, respectively,[19] the first sharp resonance (P_2: 399.4 eV) in Fig. 3(c) could be attributed to the Zn–N peak. The second peak of Zn–N overlaps with the N_2 peak (P_1: 401 eV). Peak 3 (P_3: 402.8 eV) could be attributed to the transitions of orbitals.[20] It has also been reported that, NO_2 (N(1s)$\rightarrow 2b_1$),[21] N_2O (N(1s)$\rightarrow \pi^*(N_c)$),[22] and NO (N(1s)$\rightarrow \pi^*$)[21] correspond to the band features at 403.28 eV, 404.7 eV, and 399.5 eV, respectively, and might have contributed partially to the above three peaks and the background.

3.5. The x-ray photoelectron spectroscopy

As reported by Limpijumnong *et al.*,[23] N could exist as substitutional diatomic molecules, such as NO, NC, and N_2 on the oxygen sites in ZnO wurtzite structure. The N 1s XPS spectra for ZnO films without and with Mg doping are shown in Figs. 3(d) and 3(e), respectively (after smoothing from the raw data). Without Mg doping, there is a Zn–N peak at 395.8 eV,[24] as well as $(N_2)_O$ peak[25] at around 405.30 eV. In between, there are four additional peaks visible, with the peak at 402.5 eV assigned to N–O surface contamination or N_2 trapped within the film during deposition,[26] the peak at around 400.93 eV assigned to sp^2 nitrogen bonded to three carbon neighbors,[27] the peak at around 398.05 eV assigned to C–N,[28,29] and the peak at around 399.18 eV assigned to C–H.[30]

For the N–Mg co-doped ZnO film (Fig. 3(e)), there is also a peak at around 395.54 eV assigned to Zn–N,[24] and the peaks at around 399.79 eV and 398.66 eV were assigned to –NH–,[31] C–N,[32] and N–O in the NO molecule.[33] Compared with the N-doped ZnO film without Mg, the film with Mg shows no obvious feature at the energy range higher than 402 eV, suggesting that Mg could inhibit $(N_2)_O$ production, while at the energy range from 397 eV to 402 eV, a hybridization peak arises in the film with Mg, which is split into several small peaks in the film without Mg. If atomic sensitivity factor is taken into account,[34] combining the XPS data from the N-doped ZnO and Mg–N co-doped ZnO's zinc (Fig. 3(f)), the concentration ratio of N:Zn in the Mg–N co-doped ZnO film is nearly twice that in the N-doped ZnO film, using the range from 397 eV to 402 eV. We therefore speculate that Mg promotes the inducing of N, which could have resulted in Mg–N bonding at 399.79 eV.

4. Conclusion

In summary, nitrogen-doped ZnO thin films without and with additional Mg doping were prepared using molecular beam epitaxy. *In situ* RHEED measurements reveal that nitrogen doping hinders the two-dimensional growth of ZnO. Structural characterization by XRD suggests that Mg promotes the quality growth of N-doped ZnO films with a smoother morphology as shown in AFM images. Also, XAS spectra show that the N-doped ZnO has a defect of N_O(Zn–N). In addition, XPS spectra confirm the existence of Zn–N bonding in both N-doped and N–Mg co-doped ZnO films, with the possibility that Mg inhibits $(N_2)_O$ production and may generate Mg–N bonds, which leads to the favorable increase of the N concentration.

Acknowledgment

The authors are grateful to Dr. Yufeng Zhang for helpful discussion.

References

[1] Tang Z K, Wong G K L, Yu P, Kawasaki M, Ohtomo A, Koinuma H, and Segawa Y 1998 *Appl. Phys. Lett.* **72** 3270
[2] Özgür Ü, Alivov Y I, Liu C, Teke A, Reshchikov M A, Dogăn S, Avrutin V, Cho S J and Morkoç H 2005 *J. Appl. Phys.* **98** 041301
[3] Look D C, Claflin B, Alivov Y I and Park S J 2004 *Phys. Stat. Sol. (a)* **201** 2203
[4] Walle C G V D 2000 *Phys. Rev. Lett.* **85** 1012
[5] Prze'zdziecka E, Kami'nska E, Korona K P, Dynowska E, WDobrowolski, Jakieła R, Kłopotowski Ł and Kossut J 2007 *Semi. Sci. Tech.* **22** 10
[6] Yao B, Xie Y P, Cong C X, Zhao H J, Sui Y R, Yang T and He Q 2009 *J. Phys. D: Appl. Phys.* **42** 015407
[7] Xiu F X, Yang Z, Mandalapu L J, Zhao D T and Liu J L 2005 *Appl. Phys. Lett.* **87** 152101
[8] Tang L, Wang B, Zhang Y and Gu Y 2001 *Mater. Sci. Eng. B* **176** 548
[9] Park C H, Zhang S B and Wei S H 2002 *Phys. Rev. B.* **66** 073202
[10] Gai Y Q, Yao B, Wei Z P, Li Y F, Lu Y M, Shen D Z, Zhang J Y, Zhao D X, Fan X W, Li J and Xia J B 2008 *Appl. Phys. Lett.* **92** 062110
[11] Blaha P, Schwarz K, Madsen G K H, Kvasnicka D and Luitz J 2001 *WIEN2k, An Augmented Plane Wave Plus Local Orbitals Program for Calculating Crystal Properties* (Austria: Vienna University of Technology)
[12] Perdew J P, Burke K and Ernzerhof M 1996 *Phys. Rev. Lett.* **77** 3865
[13] Bozovic I, Eckstein J N, Bozovic N A O and Krauss A R eds. 2001 *In Situ Real-Time Characterization of Thin Films* (New York: John Wiley and Sons) p. 29
[14] Chao L C, Shih Y R, Li Y K, Chen J W, Wu J D and Ho C H 2010 *Appl. Surf. Sci.* **256** 4153
[15] Sun S B, Chang X T, Li X J and Li Z J 2013 *Ceram. Int.* **39** 5197
[16] Patterson A L 1939 *Phys. Rev.* **56** 978
[17] Guo J H, Vayssieres L, Persson C, Ahuja R, Johansson B and Nordgren J 2002 *J. Phys.: Condens. Matter* **14** 6969
[18] Stöhr J, 1992 *NEXAFS Spectroscopy* (Berlin: Springer Verlag) p. 86
[19] Kapoor R and Oyama S T 1995 *Catal. Lett.* **34** 179
[20] Revel R, Bazin D, Parent P and Laffon C 2001 *Catal. Lett.* **74** 189

[21] Zhang W, Sze K H, Brion C E, Tong X M and Lee J M 1990 *Chem. Phys.* **140** 265
[22] Adachi J I, Kosugi N, Shigemasa E and Yagishita A 1995 *J. Chem. Phys.* **102** 7369
[23] Limpijumnong S, Li X, Wei S H and Zhang S B 2005 *Appl. Phys. Lett.* **86** 211910
[24] Futsuhara M, Yoshioka K and Takai O 1998 *Thin Solid Films* **322** 274
[25] Yao B, Zhang Z Z, Wang X H, Wei Z P, Li B H, Lv Y M, Fan X W, Guan LX, Xing G Z, Cong C X and Xie Y P 2006 *J. Appl. Phys.* **99** 123510
[26] Boyd K J, Marton D, Todorov S S, *et al.* 1995 *J. Vac. Sci. Technol. A* **13** 2110
[27] Quiro's C, Go'mez-García J, Palomares F J, Soriano L, Elizalde E and Sanz J M 2000 *Appl. Phys. Lett.* **77** 803
[28] Wahl B, Woke D and Makromol 1975 *Makromol. Chem.* **176** 849
[29] Yoshida T and Sawada S 1974 *Bull. Chem. Soc. Jpn.* **47** 50
[30] Souto S and Alvarez F 1997 *Appl. Phy. Lett.* **70** 1539
[31] Kannan P and John S A 2011 *Electrochim. Acta* **56** 7029
[32] Feng J, Long C, Zheng Y, Zhang F W and Fan Y D 1995 *J. Cryst. Growth* **147** 333
[33] Jeong H S and Kim C M 2007 *Bull. Korean Chem. Soc.* **28** 413
[34] Moulder J F, Stickle W F, Sobol P E and Bomben K D 1992 *Handbook of x-ray Photoelectron Spectroscopy* (Minnesota: Perkin-Elmer) p. 253